ANALYZE THE INFLUENCE OF FREQUENCIES AND SIGNALS TYPES ON GPR WAVES RESPONSES

FOUAD LAHLAL*, AHMED FAIZE, MOHAMED ATOUNTI, GAMIL ALSHARAHI

Department of Physics, Faculty of Polydisciplinary, Mohammed First University, Morocco

E-mail : f.lahlal@ump.ac.ma

ABSTRACT

The aim of this paper is analyses and study the influence of frequencies and types of pulse signals on Ground Penetrating Radar (GPR) wave's response. One of the most important steps in applying radar GPR or simulation in detecting objects buried under the surface is the frequency selection or type of signals. In this work, the effect was studied using programs (Reflexw and GprMax2d) that depend in work on the method of Finite-difference time-domain method (FDTD).

Keywords: *GPR, FDTD, frequency, pulse type, simulation, detection*

1. INTRODUCTION

Ground penetration radar (GPR) is a non-destructive geophysical tool that uses high-frequency radio waves to assess the location and depth of buried objects. Its wide range of sampling frequency combined with its non-destructive nature and its ease of implementation, has enabled it to find a large number of applications, such as archeology, construction of buildings, detection of anti-personnel mines or the analysis and characterization of stone materials. GPR provides the precise spatial location of targets from high-resolution images over short periods [1-2].

The technical design of ground penetrating radars can be classified into two groups. GPR systems that transmit a pulse and receive the reflected signal from the target are called pulsed radar, these radars generate an electromagnetic field of variable amplitude as a function of time upon emission of the pulse [3]. The pulse duration is typically between 0.5 ns and 10 ns, it depends on the type of application. However, some applications require the emission of pulses of duration up to 1μs. However, other parameters condition the duration of the pulse. Since the pulse duration is proportional to the range of the radar and inversely proportional to the spatial resolution [4]. Radars which the acquire data in the frequency domain and transmit continuously (transmitter always activated) are called CW. If the carrier is frequency modulated (FM), it is called FM-CW [5-6]. These radars are simpler in structure and therefore less expensive, but they operate much more slowly. In this work, we have simulated the operation of the pulsed radar system using different types of signals and frequencies [7].

Pulse GPR are those that acquire data in the time domain. The time pulse is transmitted and the reflected energy is received as a function of time [8]. The pulse duration is typically between 0.5 ns and 10 ns, it depends on the type of application. However, some applications require the emission of pulses of duration up to 1μs. The majority of GPR systems incorporating the pulse technique send a pulse to an antenna which produces an electromagnetic wave (EM) [6]. The characteristics of the antenna determine the center frequency of the EM wave and the associated bandwidth is determined by the pulse width. The antenna plays a major role in the dynamics of the pulsed GPR system [8].

2. MATERIAL AND METHOD

2.1 GPR principal

GPR is a device for real-time monitoring of soils and subsoils at depths that can vary from a centimeter to a few hundred meters. Its main asset is its non-destructive nature. The GPR is based on the interaction of electromagnetic waves with the heterogeneities of soils and buried objects. GPR radar systems based on the properties of electromagnetic waves are for example intended for the detection of buried objects, change of medium or for the visualization of opaque structures [9-10].

Figure1. Basic principal of GPR

2.2 Methods and software

A) FDTD method

The FDTD approach used to model GPR is a numerical method that provides a solution to Maxwell's equations, expressed in differential form in the time domain. The method, originated by Kane Yee, is based on the discretization of the partial derivatives in Maxwell's equations using central differencing [11-15].

B) Reflexw software

In this work, the collected GPR data was imported and processed using Reflexw, which is an independent package software that can import a range of different data types for the processing and interpretation of reflection and transmission data specifically in GPR application, and reflection and refraction of seismic and ultrasound data.

C) GprMax2d

GprMax2d is an open source software that simulates electromagnetic wave propagation. It uses Yee's algorithm to solve Maxwell's equations in 3D using the FDTD method. The finite difference expressions for the spatial and temporal derivatives are central-difference in nature and second-order accurate [16].

It is designed for simulating GPR and can be used to model electromagnetic wave propagation in fields such as engineering, geophysics, archaeology, and medicine. There is a wide range of applications including assessing critical infrastructures such as bridges and roads, locating buried utilities, mapping glaciers, finding anti-personnel landmines, ect [17].

3.   RADAR GPR IMPULSIONNEL

GPR is based on the emission of a short duration pulse, the pulse GPR radar is the most commonly used according to the literature and has a high commercialization rate among GPR radars. It generally consists of: a module allowing the generation of a short duration pulse, a transmitter (transmit antenna (s)), a receiver (antenna, sensor (s)), control electronics, an analog / digital converter, a sampler [18-19]. Types of signals that utilize in GPR :

A) Gaussian

In this paper we quantify such effect, showing a Gaussian Wavelet Transform [20].

A Gaussian waveform.

$$W(t)=e^{-\zeta(t-\chi)^2} \qquad (1)$$

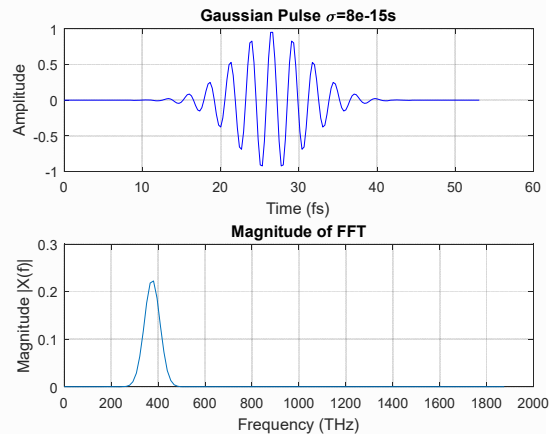where $\zeta=2\pi^2 f^2$, $\chi=1/f$ and ff is the frequency.

Figure.2. Example of the gaussian waveform

B) Ricker

The Ricker wavelet is theoretically a solution of the Stokes differential equation, which possible applicable to seismic waves propagated through viscoelastic homogeneous media. We defined the time-domain breadth and the frequency-domain bandwidth of the Ricker wavelet and developed quantities analytically in terms of the Lambert W function [21].

A Ricker (or Mexican Hat) waveform which is the negative, normalized second derivative of a Gaussian waveform.

$$W(t)=-(2\zeta(t-\chi)^2 -1)e^{-\zeta(t-\chi)^2} \qquad (2)$$

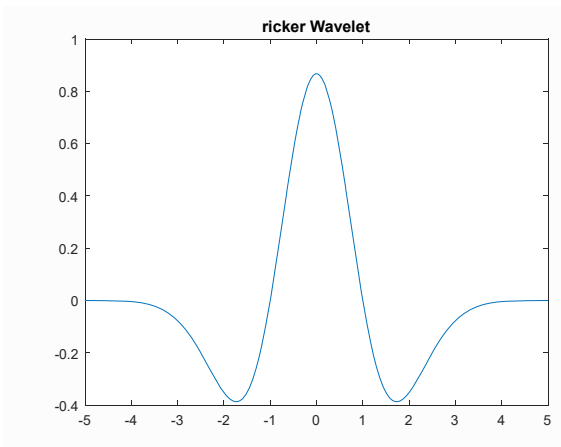where $\zeta = 2\pi 2f2$, $\chi = \sqrt{2}/f$ and f is the frequency.

Figure.3. Example of the Ricker waveform

C) Sine

A single cycle of a sine waveform.

$$W(t) = R\sin(2\pi ft) \qquad (3)$$

And

$$R = \begin{cases} 1 & \text{if } ft \leq 1, \\ 0 & \text{if } ft > 1. \end{cases}$$
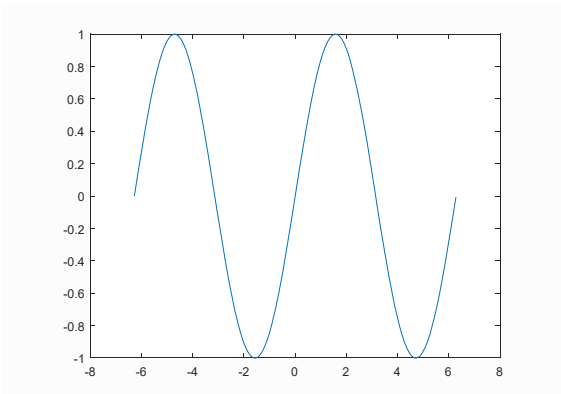
f is the frequency

Figure. 4. Example of the sine waveform

4. DEPTH RESOLUTION

The depth resolution r [m] is defined as the minimum distance between two targets so that the latter appears distinct during radar surveys. This quantity is equal to $\frac{V_e}{2B}$:

➤ V_e : is the speed of propagation in the medium,
➤ B: is the bandwidth at half height of the received signal.

Most radar systems are such that $B \sim f_c$:

$$r = \frac{3.10^8}{2.f_c\sqrt{\varepsilon_r}} \qquad (6)$$

Table 1: Relationship between frequencies, Resolution and Penetration depth

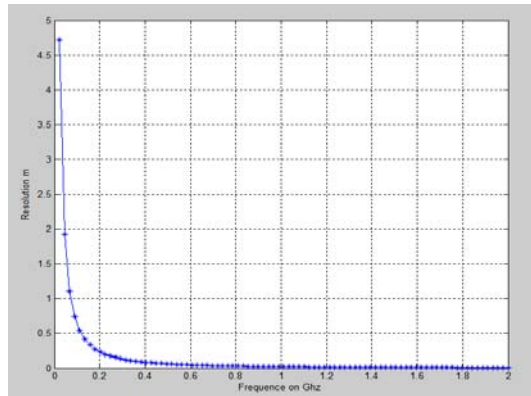| Frequency (MHz)	Resolution (cm)	Depth (M)
80	46	40
100	37	30
200	31	30
300	12	15
500	8	6
900	4	2

Figure.5. Evolution of the resolution as a function of the frequency

A higher frequency will have a shorter wavelength. Penetration is directly related to wavelength. Smaller wavelengths are more easily reflected or refracted in the superficial tissues than longer wavelengths. As the wavelength is increased (or frequency decreased) the ultrasound will penetrate deeper [22].

Wavelength

Wavelength (λ) can be described as a propagating wave which repeats itself at a particular distance and is measured in meters:

$$\lambda = \frac{2\pi}{\beta} = 2\pi\frac{\upsilon}{\omega} = \frac{\upsilon}{f} \qquad (7)$$

GPR antennas can typically be distinguished when moving along the concrete features aligned perpendicular to the direction of travel if they are spaced at least one half of a wavelength apart $\left(\frac{\lambda}{2}\right)$. Features that are stacked on top of each other can typically be distinguished if they are at least a quarter of a wavelength apart $\left(\frac{\lambda}{4}\right)$. However, features that are closer to each other than these distances may appear as a single feature in GPR data [24-25].

Relationship between frequency and depth
Choosing a frequency for a GPR survey is quite critical. The lower frequency with long wavelengths provides the deepest penetration, whereas high frequency with short wavelengths are only able to image shallow features [23].

Relationship between frequency and resolution
The resolution of subsurface features is in part affected by antenna wavelength which is also directly related to the frequency. Higher frequency radar provides higher resolution than lower frequency radar. This is due to the shorter wavelengths of high frequency produce a narrower cone of transmission, which can focus on smaller areas and thereby resolve smaller features than the more spread out transmission cones produced by low frequencies and longer wavelengths [22-23].

5.   RESULTS

To simulate the GPR signals of objects by GprMax2d, we need a certain number of parameters, such as the frequency of the antenna used, the geometry of the subsoil and targets, the dielectric permittivity, the magnetic permeability and the electrical conductivity. On a GPR image, each object below the surface appears as a hyperbola due to repeated reflections produced as the GPR unit passes over an object.
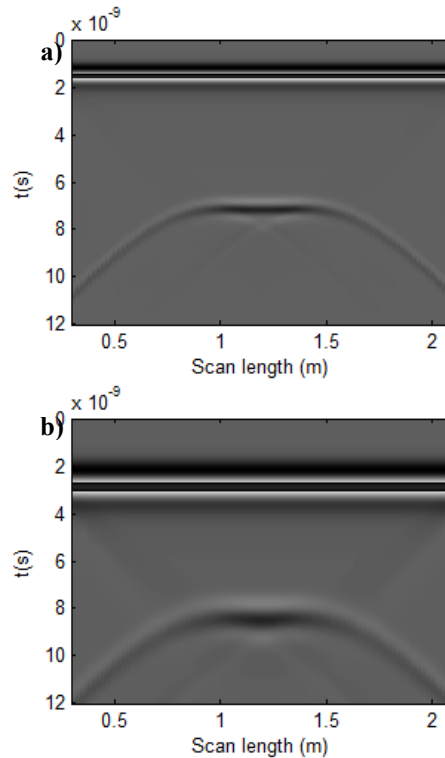
Table 2. Properties physical of materials used in simulation

Material	Relative permittivity (F/m)	Conductivity σ (S/m)
Air	1	0
Clay	12	0.001
Freshwater	81	0.0005
Iron	1.45	$9.99\ 10^6$
Wood	3	0.003
Sea water	81	4
Rock	10	0.1

5.1 Comparison between the use of frequency 400 and 800Mhz to detect the same object

In this paragraph, we will make a comparison to simulate the detection of a rectangular bar of metal using two frequencies 800 and 400MHz to find the difference and accuracy between them using the GprMax2d program. We observe through the radargrams in figure 6a and b, that the resolution of the antenna 800MHz is more than 400MHz. Also, we notice through the amplitude of the wave, it is large at a frequency of 800MHz up to 1000 A/m while with the frequency 400MHz it was less as shown in the figure 6c and d.

Figure7. Geometric profile for objects buried in the environment (iron, wood, cavity, rock and water)
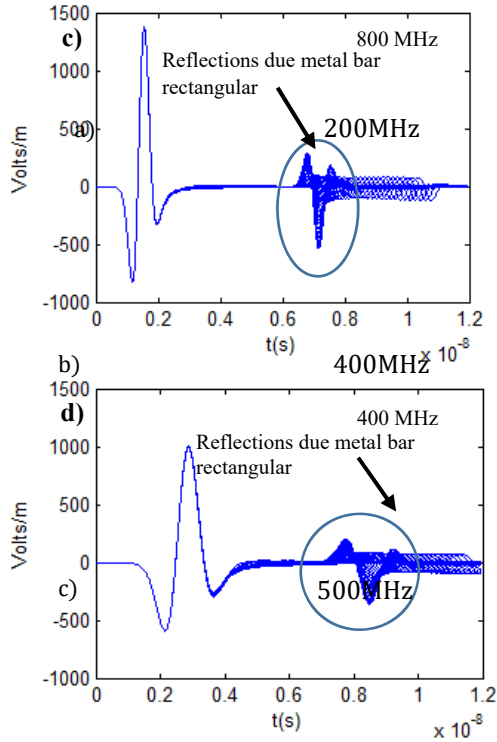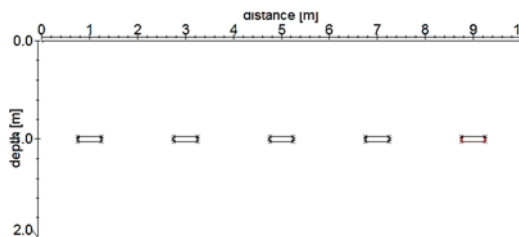

Figure.6. Model to detect a rectangular bar using two frequencies 400 and 800MHZ, (a, c) radargram and amplitude of the signal for detection bar by frequency 800 MHz respectively, (b, d) radargram and amplitude of the signal for detection bar by frequency 400 MHz respectively

5.2 Study of variation in frequencies

In this part, we will do a simulation by Reflexw software to detect five objects (Iron, wood, air, rock, water) as figure 7 and different in the physical properties as shown in table 2. Also, we will change the frequency from 200MHz to 2000MHz, note the difference in signal amplitude and form hyperbolas as shown in figure 8.
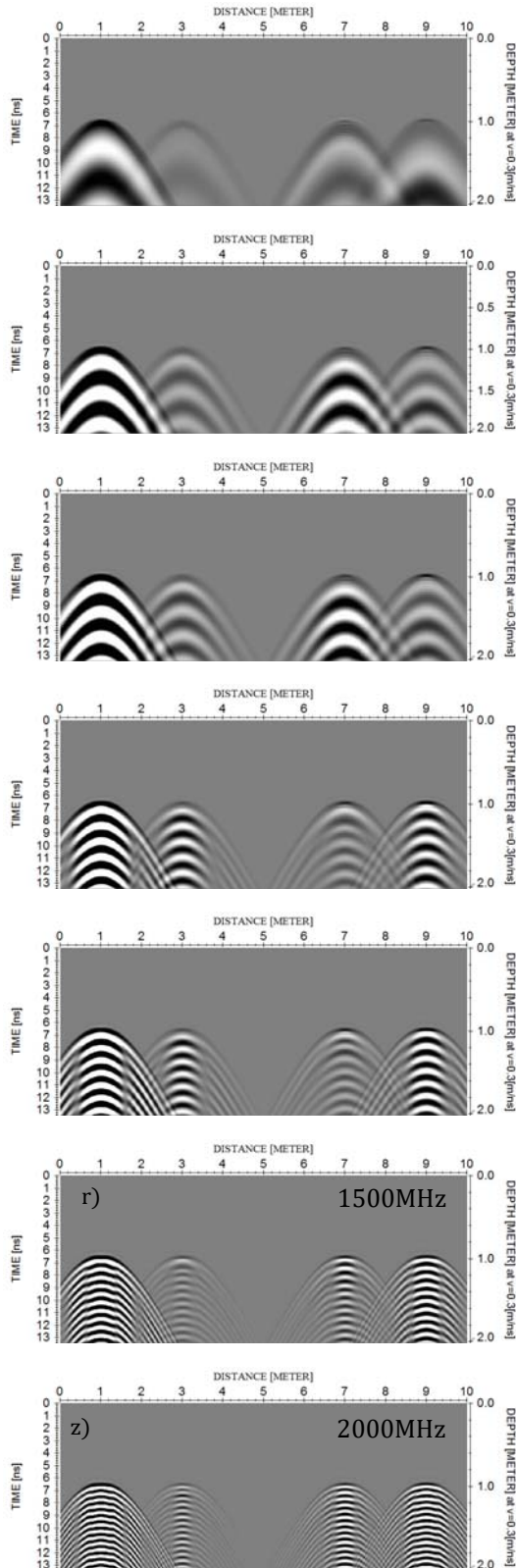
Figure. 8. Radargrams for detection the targets by
c)   *different frequencies 200-2000MHz*
                    Direct wave

5.3 Study of variation in pulse signals by GprMax2d

In this part, we will study the effect of the type of signal used by simulation by the GprMax2d program, and three types of signals as shown in figure 9, 10 and 11 (Gaussian, Ricker and Sin) at same frequency, that the radar relies on in the
d)   Direct wave
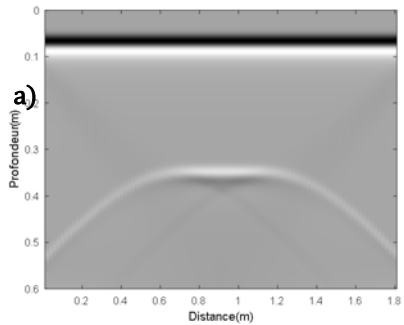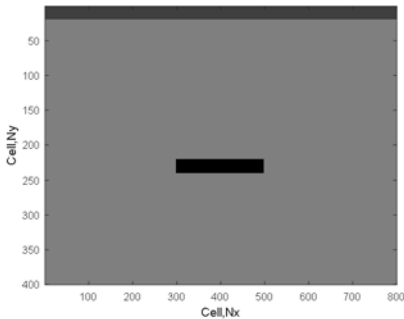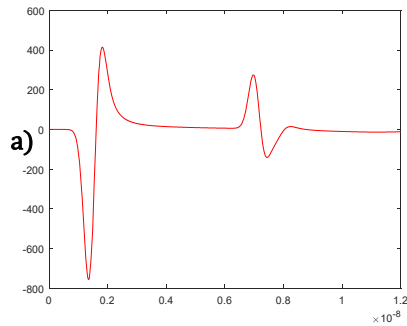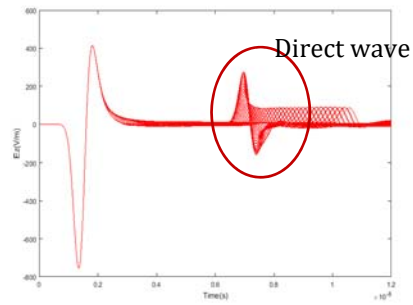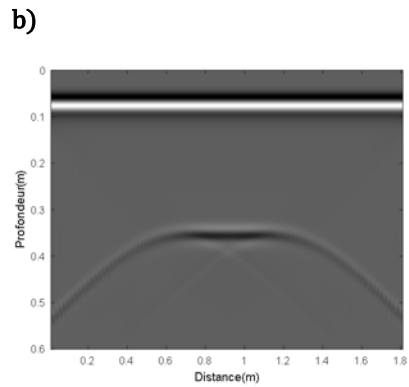process of detection and investigations were chosen.

Direct wave

a)

Figure. 9. Model for detecting a rectangular bar of metal using the Gaussian signal and frequency 800MHz, (b) radargram, (c, d) amplitude of the signal
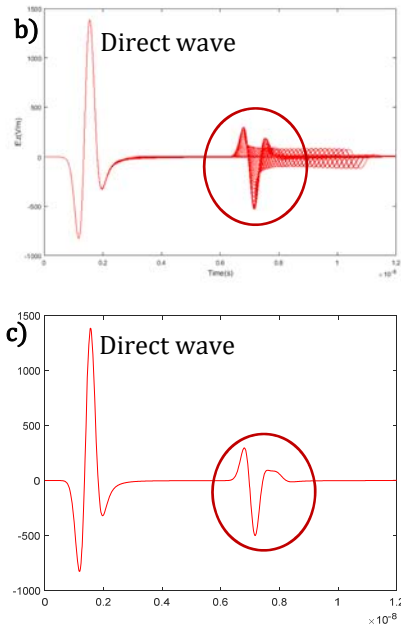
b)

a)

Figure. 10. Model for detecting a rectangular bar of metal using the Ricker signal and frequency 800MHz, (b) radargram, (c, d) amplitude of the signal
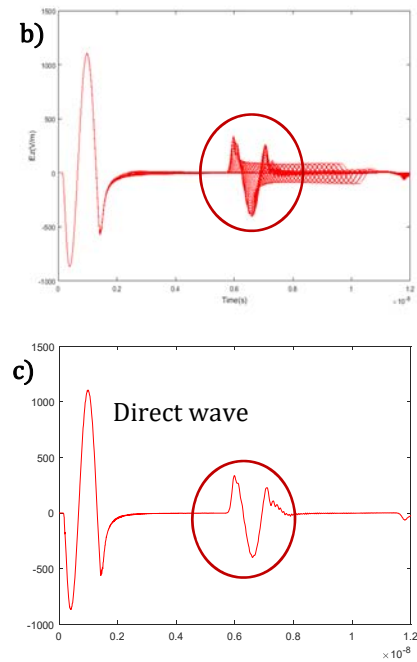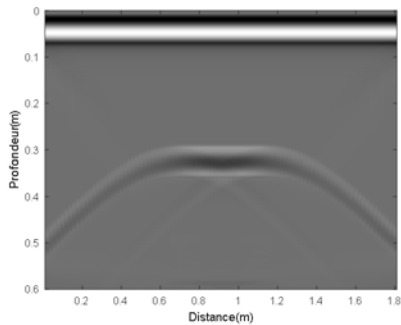

Figure. 11. Model for detecting a rectangular bar of metal using the Sin signal and frequency 800MHz, (b) radargram, (c, d) amplitude of the signal

After completing the simulation process using several pulses of the signals, it became clear that there is a difference, as is evident in the previous figures.

In the Gaussian pulse, we find that the wave amplitude reached 400 V/m and, also the reflection from the surface of the buried metal bar was different from the other (figure 9).

In the Ricker pulse, we find that the wave amplitude reached 1500 V/m and, also the reflection from the surface of the buried metal bar was different from the other (figure 10).

In the Sin pulse, we find that the wave amplitude reached 1000 V/m and, also the reflection from the surface of the buried metal bar was different from the other (figure 11).

5.4 Study of the variation in signal type by Reflexw

This model shows the signal type influence on detection targets. It is an air medium with 10m wide and 2m deep. It consists of targets rectangular bar (l = 0.3, w = 0.05) (iron, wood, air, rock and water) having different physical properties inside the

medium (ε = 1, σ = 0) at a depth of 1m from the ground surface as shown in figure 12.

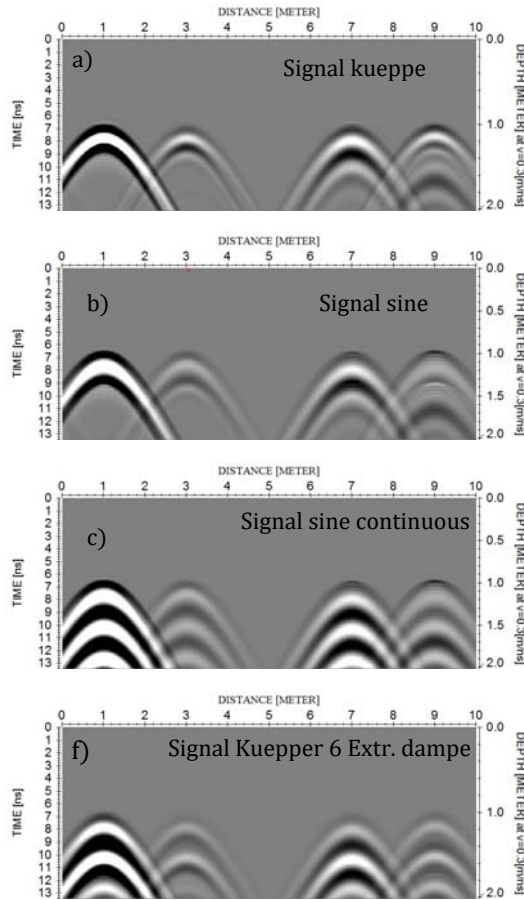Signal types: kuepper, sine, sin, sine continuous, Signal Kuepper 4 Extr. Dampe and Signal Kuepper 6 Extr. Dampe.

Figure. 12. Model for detecting five bars of metal using four signals by Reflexw software and frequency 800MHz

5.5 The difference in frequency in 3D

Comparison simulation 3D for detection of the tube using two frequencies 800 and 400MHz by using the GprMax3d. We observe through the radargrams in figure 13b, that the resolution of the antenna 800MHz is more than 400MHz as shown in the amplitude of the signal in figure 13c and e.
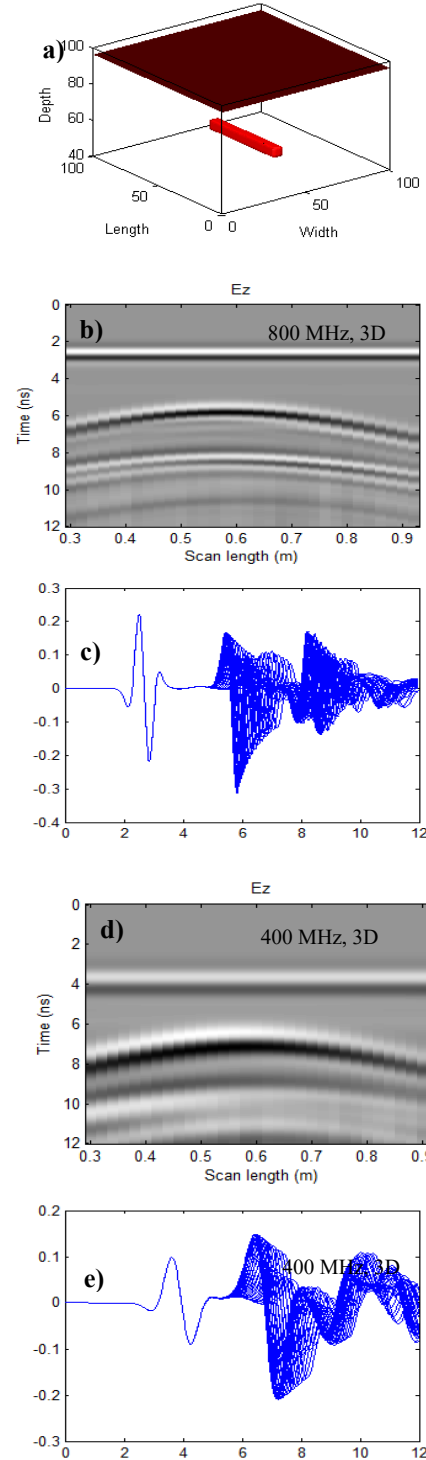

Figure. 13. (a) Model 3D to detect tube using two frequencies 400 and 800MHZ, (b, c) radargram and amplitude of the signal for detection bar by frequency 800 MHz respectively, (d, e) radargram and amplitude of the signal for detection bar by frequency 400 MHz respectively

6. CONCLUSION

The results showed that there is a large effect of the frequency in the resolution of the radar GPR and that there is a direct relation the larger the frequency the greater the resolution and also showed that there is a direct relation between the frequency and depth as the greater the frequency the decrease in depth. The results also showed that there is an effect on the type of signal used to detect objects and reflections. The results also showed the efficiency of the programs used in this work, which are based on FDTD method in simulating radar signals in detecting buried objects.

REFERENCES:

[1] DANIELS, David J. Ground penetrating radar. Encyclopedia of RF and microwave engineering, 2005.

[2] JOL, Harry M. (ed.). Ground penetrating radar theory and applications. Elsevier, 2008.

[3] H. M. Jol, "Ground Penetrating Radar: Theory and Applications", First edition 2009 ed., Elsevier Science, 2009.

[4] D. Daniels, "Surface-penetrating radar", British Library Cataloguing in Publication Data, 1996.

[5] R. Perez, "Contribution à l'analyse théorique et expérimentale de radargrammes GPR. Performances des antennes : apports d'une configuration multistatique", thèse de doctorant, Université de Limoges, 2005.

[6] F. Rejiba, "Modélisation de la propagation des ondes électromagnétiques en milieux hétérogènes : Application au Radar Sol.", thèse de doctorat, Université Pierre et Marie Curie - Paris VI, 2002.

[7] Warren, Craig, Giannopoulos, Antonios, et Giannakis, Iraklis. gprMax: Open source software to simulate electromagnetic wave propagation for Ground Penetrating Radar. Computer Physics Communications, 2016, vol. 209, p. 163-170.

[8] Alsharahi, G., Faize, A., Maftei, C., Bayjja, M., Louzazni, M., Driouach, A., Khamlichi, A. (2019). Analysis and modeling of GPR signals to detect cavities: Case Studies in Morocco. Journal of Electromagnetic Engineering and Science, 19, 177-187.

[9] Alsharahi, G., Faize, A., Louzazni, M., Mostapha, A.M.M., Bayjja, M., Driouach, A. (2019). Detection of cavities and fragile areas by numerical methods and GPR application. Journal of Applied Geophysics, 164, 225-236.

[10] TJORA, Sigve, EIDE, Egil, et LUNDHEIM, Lars. Evaluation of methods for ground bounce removal in GPR utility mapping. In : Proceedings of the Tenth International Conference on Grounds Penetrating Radar, 2004. GPR 2004. IEEE, 2004. p. 379-382.

[11] Alsharahi, G., Mostapha, A.M.M., Faize, A., Driouach, A. (2016). Modelling and simulation resolution of ground-penetrating radar antennas. Journal of Electromagnetic Engineering and Science, 16(3), 182-190.

[12] GUREL, Levent et OGUZ, Ugur. Three-dimensional FDTD modeling of a ground-penetrating radar. IEEE Transactions on Geoscience and Remote Sensing, 2000, vol. 38, no 4, p. 1513-1521.

[13] Giannakis, I., Giannopoulos, A., Warren, C. (2016). A Realistic FDTD Numerical Modeling Framework of Ground Penetrating Radar for Landmine Detection. IEEE Journal of Selected Topics in Applied Earth Observations and Remote Sensing, 9(1), 37-51.

[14] Howlader, M.O.F., Sattar, T.P. (2015). FDTD based numerical framework for ground penetrating radar simulation. Progress In Electromagnetics Research M, 44, 127-138.

[15] Shangguan, P., Al-Qadi, I.L. (2015). Calibration of FDTD simulation of GPR signal for asphalt pavement compaction monitoring. IEEE Transactions on Geoscience and Remote Sensing, 53(3), 1538-1548.

[16] Giannopoulos, A. (2005). Modelling ground penetrating radar by GprMax, Construction and Building Materials, 19(10), 755-762.

[17] Feng, D.-S., Chen, J.-W., Wu, Q. (2014). A hybrid ADI-FDTD subgridding scheme for efficient GPR simulation of dispersion media. Acta Geophysica Sinica, 57(4), 1322-1334.

[18] Benedetto, A., Tosti, F., Pajewski, L., D'Amico, F., Kusayanagi, W. (2014). FDTD simulation of the GPR signal for effective inspection of pavement damages. In Proceedings of the 15th International Conference on Ground Penetrating Radar, GPR 2014, 513-518.

[19] De Domenico, D., Campo, D., Teramo, A. (2013). FDTD modelling in high-resolution 2D and 3D GPR surveys on a reinforced concrete column in a double wall of hollow bricks. Near Surface Geophysics, 11(1), 29-40.

[20] NAVARRO, Rafael et TABERNERO, Antonio. Gaussian wavelet transforms: two alternative fast implementations for images. Multidimensional Systems and Signal Processing, 1991, vol. 2, no 4, p. 421-436.

[21] LIU, Jianlei, WU, Yafei, HAN, Dehua, et al. Time-frequency decomposition based on Ricker wavelet. In : SEG Technical Program Expanded Abstracts 2004. Society of Exploration Geophysicists, 2004. p. 1937-1940.

[22] DAVIS, J. L♯ et ANNAN, A. Peter. Ground-penetrating radar for high-resolution mapping of soil and rock stratigraphy 1. Geophysical prospecting, 1989, vol. 37, no 5, p. 531-551.

[23] PÉREZ-GRACIA, Vega, DI CAPUA, Daniel, GONZÁLEZ-DRIGO, Ramón, et al. Laboratory characterization of a GPR antenna for high-resolution testing: Radiation pattern and vertical resolution. NDT & E International, 2009, vol. 42, no 4, p. 336-344.

[24] BACHRACH, Ran et NUR, Amos. Same wavelength GPR and ultra-shallow seismic reflection on a river point bar: Sand stratigraphy and water table complexity. In : SEG Technical Program Expanded Abstracts 1998. Society of Exploration Geophysicists, 1998. p. 840-843.

[25] NOON, David A., STICKLEY, Glen F., et LONGSTAFF, Dennis. A frequency-independent characterisation of GPR penetration and resolution performance. Journal of Applied Geophysics.